Synchronization of Oscillating Reactions in an Extended Fluid System

M. S. Paoletti, C. R. Nugent, and T. H. Solomon*

Department of Physics, Bucknell University, Lewisburg, PA 17837

(Dated: February 17, 2006)

Abstract

We present experiments on the synchronization of a dynamical, chemical process in an extended, flowing, fluid system. The oscillatory Belousov-Zhabotinsky (BZ) chemical reaction is the process studied, and the flow is an annular chain of counter-rotating vortices. Azimuthal motion of the vortices is controlled externally, enabling us to vary the type of transport. We find that oscillations of the BZ reaction synchronize throughout the extended fluid system only if transport in the flow is superdiffusive, with tracers in the flow undergoing rapid, distant jumps called Lévy flights.

Synchronization phenomena are significant in a wide range of systems such as neural networks[1], Josephson junctions[2], biological oscillators[3], and the Global Positioning System[4]. For discrete networks, it has been shown that synchronization is enhanced when different parts of the system are coupled via a combination of short- and long-range connections ("small-world" networks[5]). But collective behavior and synchronization are significant in many continuous systems as well, such as spawning cycles for phytoplankton in the ocean[6], oscillations in yeast cell populations in a fluid mixer[7], and ozone cycles in the atmosphere[8]. Synchronization via fluid mixing in continuous systems has only recently received attention theoretically[9–13], and experimental studies are lacking. Furthermore, synchronization has not been considered for *extended* fluid systems whose sizes are much larger than characteristic length scales of the flow.

In this Letter, we show experimentally that the key to synchronization of a dynamical chemical process in an extended, flowing, fluid system is superdiffusive transport. Superdiffusion is characterized by tracers undergoing "Lévy flight" trajectories[14, 15], which are jumps between distant regions in the flow. Similar to "short-cuts" in a discrete, small-world network, Lévy flights provide long-range mixing. The experiments consist of the oscillatory Belousov-Zhabotinsky reaction [16, 17] in an annular chain of counter-rotating vortices. Motion of the vortex chain in the azimuthal direction is controlled externally, enabling us to vary the transport between diffusive and superdiffusive regimes.

Synchronization of dynamical processes in fluid systems has only recently received attention. To our knowledge, there has been only one experimental study of synchronization in a continuous fluid system[18]; however, that study deals with a stagnant fluid system with no mixing. Recent theoretical studies have shown that chaotic fluid mixing can synchronize systems whose size is comparable to the characteristic flow length scale[9–13]. For larger-scale fluid systems, though, it is necessary to consider long-range transport to understand the collective behavior. Transport is analyzed by considering the variance of a spreading distribution of tracers: $\langle x^2 \rangle \sim t^\gamma$. If the growth exponent $\gamma = 1$, then the transport is diffusive; transport with $\gamma > 1$ is termed superdiffusive. Diffusive transport, whether molecular (due to Brownian motion) or enhanced (due to chaotic mixing[19, 20]), is a local process that typically occurs on time-scales far too long to synchronize distant parts of an extended system. However, if the transport is superdiffusive, tracers in the flow undergo Lévy flight trajectories[14, 15], which provide mixing between distant parts of the system.

2
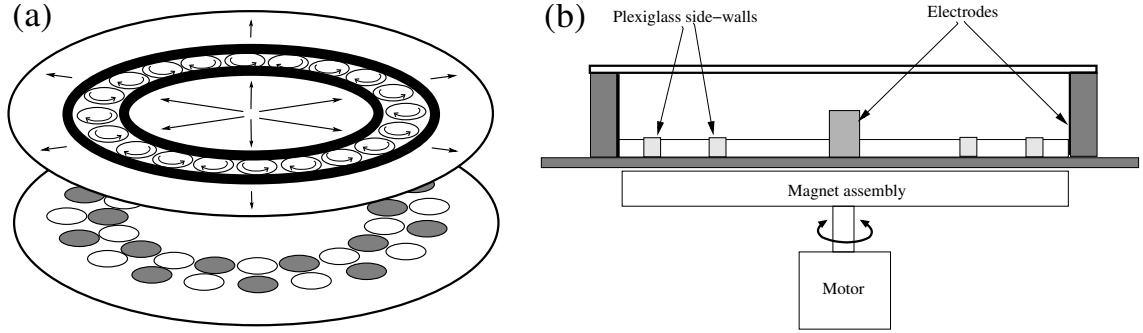
FIG. 1: Apparatus and flow. (a) Exploded view of magnetohydrodynamic forcing, along with the resulting annular ring of vortices. The lower layer shows the magnet arrangement, with shaded and unshaded circles showing magnets with N or S side up. The radial arrows in the upper layer show the driving electrical current. (b) Side view of experimental apparatus. A cylindrical container above the magnet assembly holds the fluid, along with two concentric plexiglass rings, a center electrode and an outer ring electrode. The magnet assembly is mounted on a motor whose motion can be controlled precisely. The fluid layer is 2 mm thick, and the annular chain has inner and outer radii 6.1 and 8.3 cm.

The experimental flow is generated using a magnetohydrodynamic technique (Fig. 1)[21]. A radial current passing through a thin electrolytic solution interacts with a spatially-periodic magnetic field produced by an assembly of magnets mounted coaxially on a motor below the fluid layer. The resulting flow is a chain of 20 counter-rotating vortices, wrapped into an annulus[22]. The fluid is composed of the chemicals used for the Belousov-Zhabotinsky (BZ) reaction[23], a nonlinear reaction well-known for its oscillatory and sometimes chaotic behavior. The chemical reaction occurring *within each vortex* oscillates blue-red in an almost (but not quite) periodic fashion, and coupling between different parts of the system is determined by fluid transport between vortices.

Time dependence of the vortex chain is controlled externally with the motor and magnet assembly. If the motor is off, the flow is time-independent and the vortices are stationary. For time-dependent flows, the motor (and vortices) is programmed to move in the azimuthal direction with a superposition of oscillatory and constant velocity (drifting) components, as described below. Except where noted, the frequency of imposed oscillatory component of the flow time-dependence is 25 mHz.

Numerical modelling is used to gain insight into the transport properties of this flow. A simplified model of the flow is used, based on well-known equations for the velocity field of a chain of counter-rotating vortices[24]:

$$\dot{x} = -U \cos(kx_s) \sin(ky) \tag{1}$$

$$\dot{y} = U \sin(kx_s) \cos(ky) \tag{2}$$

$$x_s = x + \frac{v_o}{\omega} \sin(\omega t) + v_d t \tag{3}$$

where the vortex width and height equal π/k where k is the wavenumber. In this model, the vortices are arranged in a linear chain rather than in an annulus; x and y are analogous to the angular and radial coordinates in the experiment. The vortex chain moves in the x-direction, drifting with velocity v_d and oscillating with angular frequency ω and maximum velocity v_o. Transport in the oscillating vortex chain (i.e., with $v_d = 0$) has been studied extensively[19, 20, 25, 26]; the drift term, however, is new and is added to model (phenomenologically) the imposed drift in the experiments. Throughout the paper, the drift and oscillation velocities v_d and v_o are normalized by the maximum flow velocity U (0.65 cm/s for experiments). If $v_o = 0$, tracers in the flow move either in closed paths within the vortex cores or in a jet region that snakes around and between the vortices.

The transport behavior is illustrated with Poincaré sections, determined numerically (Eqs. 1-3) by plotting the location of one or more tracers in the flow once every period of oscillation. If $v_o \neq 0$, the system is typically divided into ordered and chaotic regions (Figs. 2a and b). If $v_d > v_o$, transport is typically superdiffusive. In most cases, there are two chaotic regions, separated by an ordered region in the middle of the jet (light blue in Fig. 2a). Tracers in the chaotic regions (dark red or blue in Fig. 2a) "stick" temporarily to this ordered region and to ordered regions in the vortex cores (purple and green in Fig. 2a), mimicking the behavior in those regions. The result is Lévy flights where the tracers alternate between circling within a vortex and flying around the annulus, producing superdiffusive transport ($\gamma > 1$). For the case shown in Fig. 2a, the ordered region in the jet also prevents mixing between adjacent vortices. In some cases, there is only one chaotic region, but there are ordered "islands" which produce long-range flights[26] (some of the smaller white regions in Fig. 2b). Transport is still superdiffusive, although there is no barrier preventing mixing between adjacent vortices. For $v_d < v_o$, Poincaré sections look similar to Fig. 2b, except that islands that produce long-range flights are absent. Transport in this case is diffusive
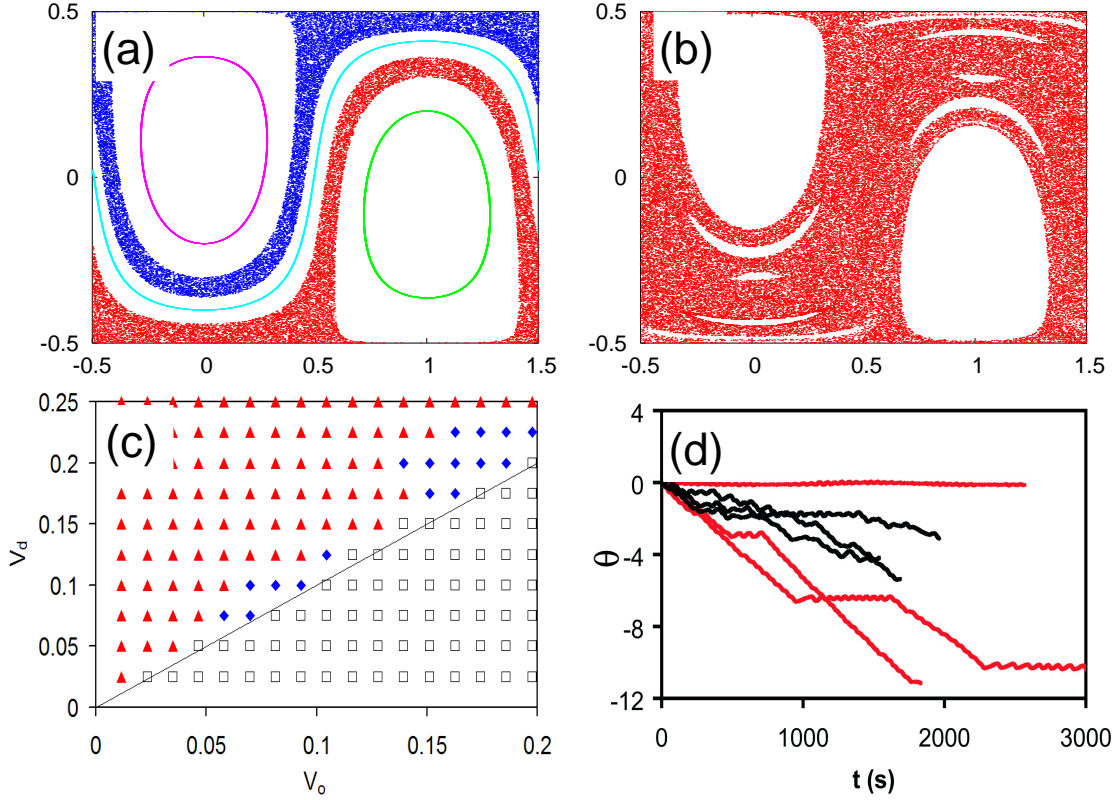
FIG. 2: Transport properties of oscillating/drifting vortex chain. (a) Numerically determined Poincaré section for $v_o = 0.070$ and $v_d = 0.150$. Different colors are used to denote different tracers in the flow; the dark blue and red dots correspond to two separate chaotic regions, the purple and green dots correspond to ordered regions in the vortex cores, and the light blue dots correspond to an ordered region that snakes around and between vortices. The labelled numbers are the x- and y-coordinates in units of one vortex width. (b) Poincaré section for $v_o = 0.174$ and $v_d = 0.225$. Only one trajectory is used for this plot; the dots show one connected chaotic region, while the white regions are ordered regions. (c) Parameter space plot. The red triangles correspond to cases with two separate chaotic regions (as in (a)), the open squares correspond to one unified chaotic region with no flight-producing islands, and the blue diamonds correspond to one unified chaotic region containing flight-producing islands (i.e., those with flights of at least 20 vortex widths, as in (b)). (d) Angular displacement (in radians) for sample experimental trajectories. The red curves ($v_o = 0$, $v_d = 0.060$) show flight behavior ($\gamma = 1.8$) and the black curves ($v_o = 0.060$ and $v_d = 0.060$, $f = 15$ mHz) corresponds to almost-diffusive behavior ($\gamma = 1.2$). For both cases in (d), the maximum flow velocity is 0.43 mm/s.

5

assuming no resonances[25, 26] and mixing is predominately between adjacent vortices. The numerical results are summarized in a parameter space diagram shown in Fig. 2c.

Figure 2d shows the angular displacement for several experimental trajectories. The red curves are Lévy flights, alternating between sticking within vortices and moving rapidly between distant parts of the system. The result is rapid separation of typical trajectories. An exponent $\gamma = 1.8$ is measured for transport in this experiment, indicating superdiffusion. The black curves show typical experimental trajectories for $v_d = v_o$; an exponent $\gamma = 1.2$ is found, consistent with this condition as the boundary between diffusion and superdiffusion.

Experiments on the oscillatory BZ chemical reaction use the counter-rotating vortex flow discussed above; the dynamics of the BZ reaction do not have any measurable effect on the flow. Synchronization of the reaction is quantified by the Kuramoto order parameter[27] $r = \left| \frac{1}{N} \sum e^{i\phi_n} \right|$ where $N = 20$ is the number of vortices, n denotes an individual vortex, and ϕ_n is the phase of the BZ oscillation determined by the summed intensities for that vortex. For all BZ experiments, the system is allowed to desynchronize before any time-dependence is initiated. A run is classified as "synchronized" if r reaches a minimum value of 0.95. For some cases, the system maintains synchronization indefinitely; however, there are cases where the system alternates between synchronized and unsynchronized states.

Sequences of images of the BZ reaction are shown in Fig. 3, along with corresponding plots of r in Fig. 4. If the vortices are stationary, mixing between vortices is purely via molecular diffusion which is too weak to produce synchronization (blue curve in Fig. 4a) – the BZ reaction in each vortex oscillates in an almost-periodic manner with average frequencies that vary from one vortex to the next. In fact, even if the system starts fully synchronized, the BZ oscillations desynchronize rapidly if $v_d = v_o = 0$. For oscillatory time dependence with $v_d < v_o$, mixing between vortices is greatly enhanced by chaotic mixing but is still diffusive and local, i.e., between neighboring vortices. In this case, the BZ oscillations spontaneously forms waves (Fig. 3a and red curve in Fig. 4a) but are unable to oscillate in unison throughout the entire system. The waves evolve in time in a complicated, non-periodic manner.

If $v_d > v_o$, transport is typically superdiffusive and the BZ oscillations synchronize. Two different states are observed. In most cases, "co-rotating" synchronization is found (Figs. 3b and 4b) in which the BZ reaction in even and odd vortices synchronize independently with arbitrary phases. There are also cases where the system synchronizes globally, with

6
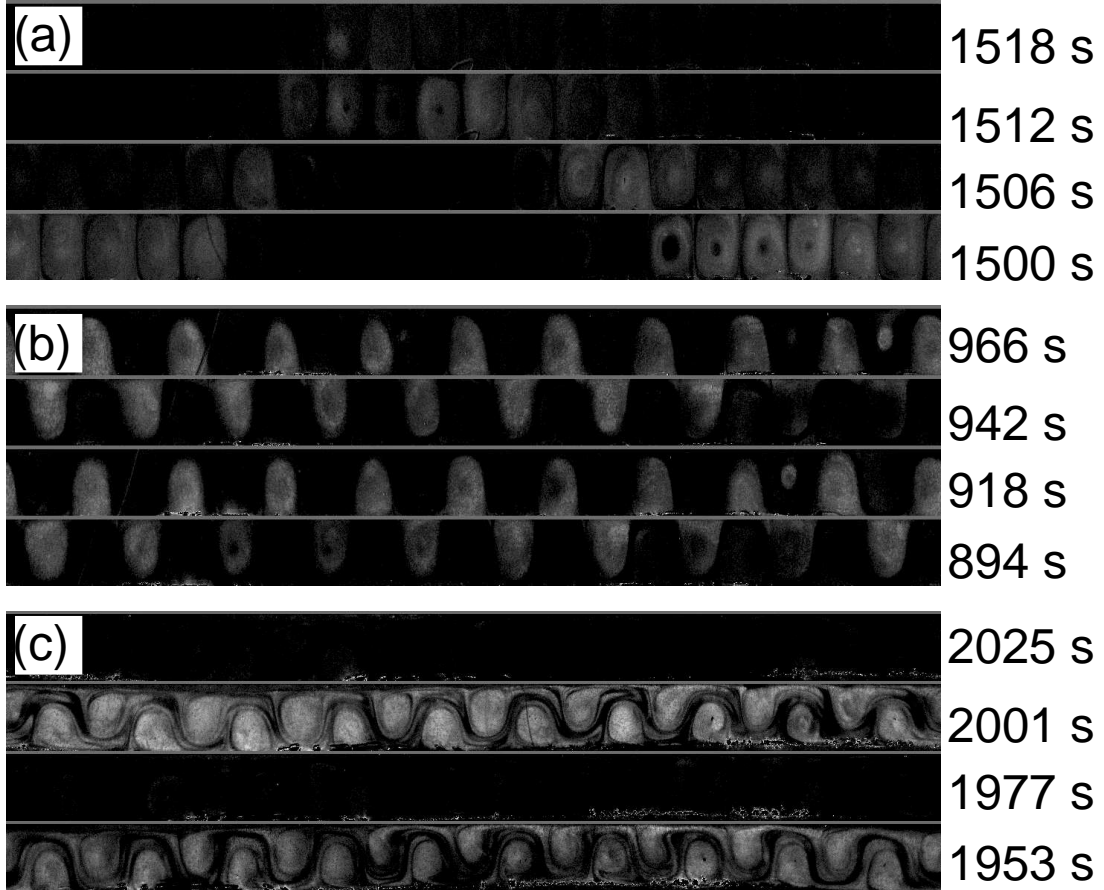
FIG. 3: Sequences of images showing dynamics of the Belousov-Zhabotinsky reaction in the vortex chain. All of the images are decurled and dedrifted; i.e., the annulus of vortices is straightened into a strip (with periodic boundary conditions), and the reference frame moves with the vortices. Times are from the beginning of the run. (a) Wave behavior; $v_o = 0.081$, $v_d = 0$. (b) Co-rotating synchronization; $v_o = 0.020$, $v_d = 0.097$. The phase difference between the two chains is 180° for this case, but it is arbitrary in general. (c) Global synchronization; $v_o = 0.151$, $v_d = 0.222$.

the BZ reaction in every vortex oscillating in unison (Fig. 3c and black curve in 4a).

The experimental reaction dynamics are summarized with a parameter space diagram (Fig. 4c) that can be compared with the numerically-determined transport behavior (Fig. 2c). Three types of behavior are apparent in both diagrams. (1) For $v_d < v_o$ (below the diagonal line in both Fig. 2c and 4c), the transport is diffusive, and the BZ reaction remains unsynchronized, although waves typically form. (2) For $v_d > v_o$, transport is superdiffusive but mixing between adjacent vortices is blocked in most cases, resulting in co-rotating syn-

7
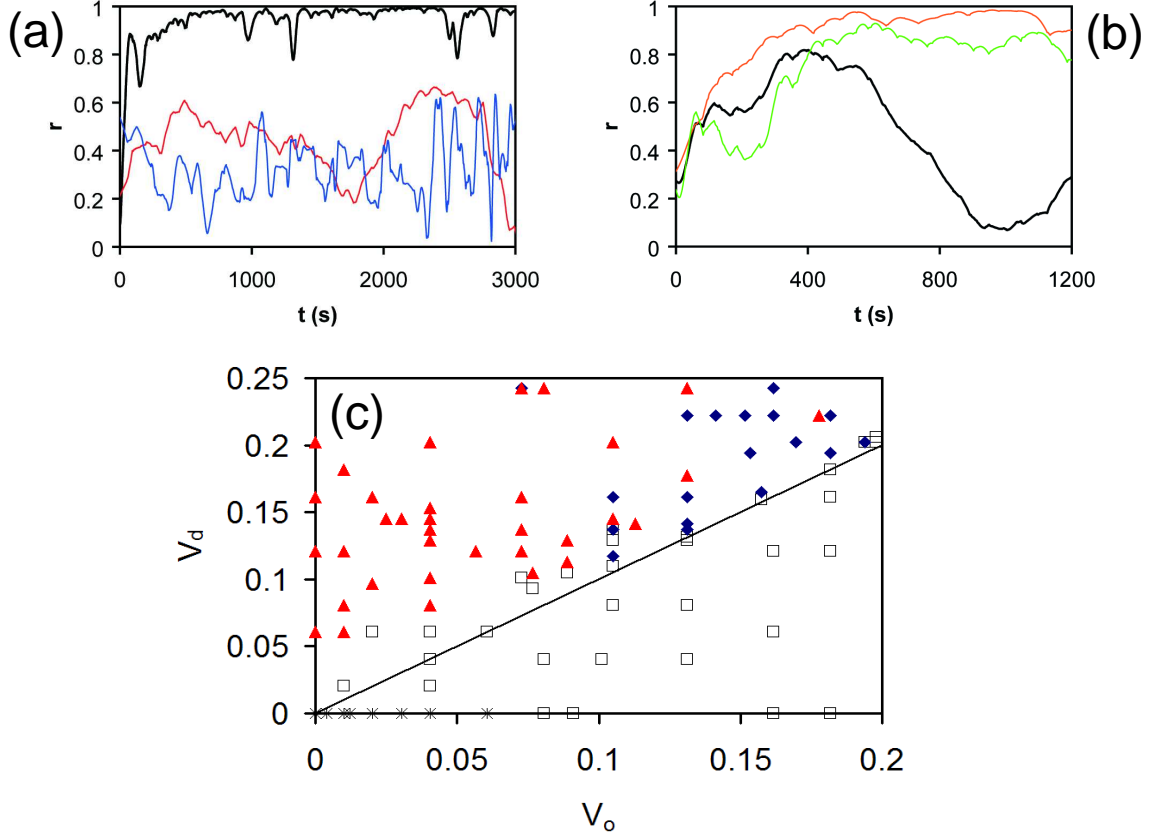
FIG. 4: Synchronization experiments. (a) Kuramoto order parameter r for unsynchronized case ($v_o = v_d = 0$, blue curve), wave behavior from Fig. 3a ($v_o = 0.081$, $v_d = 0$, red curve), and global synchronization from Fig. 3c ($v_o = 0.151$, $v_d = 0.222$, black curve). (b) Kuramoto order parameter for co-rotating synchronization from Fig. 3b ($v_o = 0.020$, $v_d = 0.097$); global parameter (black curve) and order parameter calculated only for odd and even vortex chains (orange and green curves). (c) Parameter diagram showing global synchronization (blue diamonds), co-rotating synchronization (red triangles), wave behavior (open black squares) and completely decorrelated (black asterisks).

chronization for the BZ reaction. There is a small deviation from the line $v_d = v_o$, due to decreased long-range transport for small v_o and v_d. (3) There are cases for $v_d > v_o$ where transport is superdiffusive but with one chaotic region allowing mixing between adjacent vortices, resulting in global synchronization of the BZ oscillations.

A few issues need to be considered when interpreting these results. First, Lévy flights are not instantaneous. Any theoretical analysis of synchronization in an extended flow

8

must compare the flight times to reaction timescales. Second, although mixing due to flights is analogous to short-cuts in a discrete small-world network, there are differences. Lévy flights are not random; they allow fluid in a vortex to mix with all other vortices in the system (neglecting barriers). The strength of this mixing depends on the size of the ordered regions (Fig. 2) and the jump length distribution for the flights[14, 15]. Third, stability of the synchronized state needs to be considered; even though the system can achieve synchronization from an initially-unsynchronized state (when transport is superdiffusive), synchronization is not always maintained once achieved. Finally, it would be interesting to see if these results hold even for aperiodic oscillators, e.g., with the chaotic BZ reaction.

Summarizing, we find that Lévy flights and superdiffusive transport play a crucial role in synchronizing an oscillatory reactive process in a flowing fluid system over distances larger than the characteristic length scale of the flow (a vortex width in this case). The results of these experiments could shed light on various processes occurring in atmospheric, oceanic, industrial and biological fluid systems. Superdiffusive transport is often present in flowing dynamical systems, however the effects of the transport properties have yet to be investigated. This result could also be applied to understanding dynamics of networks with a large number of mobile nodes; e.g., disease outbreaks in large populations. Rather than attempting to characterize the network traditionally by determining how the nodes are "connected" (a difficult task for large, mobile networks), it may be simpler to approximate the large discrete system as a continuous fluid system. Dynamics then could be predicted by determining whether transport in the "fluid" is diffusive or superdiffusive.

————————

* email address: `tsolomon@bucknell.edu`

[1] M. Diesmann, M. O. Gewaltig, and A. Aertsen, Nature **402**, 529 (1999).

[2] B. R. Trees, V. Saranathan, and D. Stroud, Phys. Rev. E **71**, 016215 (2005).

[3] A. T. Winfree, *The Geometry of Biological Time* (Springer, New York, 1980).

[4] T. Bahder, Phys. Rev. D **68**, 063005 (2003).

[5] D. J. Watts and S. H. Strogatz, Nature **393**, 440 (1998).

[6] G. A. Tarling and J. Cuzin-Roudy, Limnol. Oceanogr. **48**, 2020 (2003).

[7] S. Dano, F. Hynne, S. D. Monte, F. d'Ovidio, P. G. Sorensen, and H. Westerhoff, Faraday Discuss. **120**, 261 (2001).

[8] D. G. Tan, G. H. Haynes, P. H. MacKenzie, and J. Pyle, J. Geophys. Res. **103**, 1585 (1998).

[9] T. Tel, A. de Moura, C. Grebogi, and G. Karolyi, Phys. Rep. **413**, 91 (2005).

[10] G. Karolyi, A. Pentek, Z. Toroczkai, T. Tel, and C. Grebogi, Phys. Rev. E **59**, 5468 (1999).

[11] G. Karolyi, A. Pentek, I. Scheuring, T. Tel, and Z. Toroczkai, Proc Nat. Acad. Sci. **25**, 13661 (2000).

[12] Z. Neufeld, Phys. Rev. Lett. **87**, 108301 (2001).

[13] Z. Neufeld, I. Z. Kiss, C. S. Zhou, and J. Kurths, Phys. Rev. Lett. **91**, 084101 (2003).

[14] M. F. Schlesing, G. M. Zaslavsky, and J. Klafter, Nature **363**, 31 (1993).

[15] T. H. Solomon, E. R. Weeks, and H. L. Swinney, Phys. Rev. Lett. **71**, 3975 (1993).

[16] A. T. Winfree, Science **175**, 634 (1972).

[17] R. J. Field and M. Burger, *Oscillations and Traveling Waves in Chemical Systems* (Wiley, New York, 1985).

[18] M. Tinsley, J. X. Cui, F. V. Chirila, A. Taylor, S. Zhong, and K. Showalter, Phys. Rev. Lett. **95**, 038306 (2005).

[19] T. H. Solomon and J. P. Gollub, Phys. Rev. A **38**, 6280 (1988).

[20] R. Camassa and S. Wiggins, Phys. Rev. A **43**, 774 (1991).

[21] H. Willaime, O. Cardoso, and P. Tabeling, Phys. Rev. E **48**, 288 (1993).

[22] M. S. Paoletti and T. H. Solomon, Euro. Phys. Lett. **69**, 819 (2005).

[23] C. R. Nugent, W. M. Quarles, and T. H. Solomon, Phys. Rev. Lett. **93**, 218301 (2004).

[24] S. Chandresekhar, *Hydrodynamic and Hydromagnetic Stability* (Clarendon, Oxford, 1961).

[25] P. Castiglione, A. Crisanti, A. Mazzino, M. Vergassola, and A. Vulpiani, J. Phys. A **31**, 7197 (1998).

[26] T. H. Solomon, A. T. Lee, and M. A. Fogleman, Physica D **157**, 40 (2001).

[27] Y. Kuramoto, *Chemical Oscillations, Waves and Turbulence* (Springer, Berlin, 1984).